

SA-MLP: Enhancing Point Cloud Classification with Efficient Addition and Shift Operations in MLP Architectures

Qiang Zheng¹, Chao Zhang¹, Jian Sun¹,

Abstract

This study addresses the computational inefficiencies in point cloud classification by introducing novel MLP-based architectures inspired by recent advances in CNN optimization. Traditional neural networks heavily rely on multiplication operations, which are computationally expensive. To tackle this, we propose Add-MLP and Shift-MLP, which replace multiplications with addition and shift operations, respectively, significantly enhancing computational efficiency. Building on this, we introduce SA-MLP, a hybrid model that intermixes alternately distributed shift and adder layers to replace MLP layers, maintaining the original number of layers without freezing shift layer weights. This design contrasts with the ShiftAddNet model from previous literature, which replaces convolutional layers with shift and adder layers, leading to a doubling of the number of layers and limited representational capacity due to frozen shift weights. Moreover, SA-MLP optimizes learning by setting distinct learning rates and optimizers specifically for the adder and shift layers, fully leveraging their complementary strengths. Extensive experiments demonstrate that while Add-MLP and Shift-MLP achieve competitive performance, SA-MLP significantly surpasses the multiplication-based baseline MLP model and achieves performance comparable to state-of-the-art MLP-based models. This study offers an efficient and effective solution for point cloud classification, balancing performance with computational efficiency.

Keywords: Point Cloud, Classification, Shift, Addition, Computational Efficiency

1. Introduction

The analysis of point cloud data has become an essential task in numerous applications, including autonomous driving [1, 2], robotics [3, 4], and virtual reality [5, 6]. Unlike traditional 2D images, point clouds present unique challenges due to their irregular and sparse nature, which complicates the direct application of conventional neural network (CNN) architectures. Recent advances in deep learning, such as multi-layer perceptrons (MLPs), CNNs, and Transformers, have shown promise in processing point cloud data effectively [7, 8, 9]. However, the computational inefficiencies inherent in these models, primarily due to their reliance on multiplication operations, present significant barriers to real-time applications and deployment on resource-constrained devices .

Traditional neural networks depend heavily on multiplication operations within their layers, leading to high computational costs. Multiplicative operations require more clock cycles and consume more energy compared to simpler operations like addition or bit shifting. This inefficiency becomes particularly pronounced in large-scale models or those intended for deployment on edge devices. As a result, the search for alternatives to multiplication in neural network layers has gained momentum, with recent studies exploring the replacement of multiplication with more efficient operations such as addition and shift [10, 11, 12]. Given the increasing demand for efficient computation, optimizing the operations within neural networks has become critical. In this context, the present study aims to develop novel MLP-based architectures that leverage addition and shift operations to replace multiplications, thereby enhancing computational efficiency while maintaining or even improving classification performance on point cloud data.

In recent years, several studies have focused on optimizing CNNs by reducing the reliance on multiplication operations. AdderNet [10], for instance, replaces multiplications with additions in CNNs, leading to a significant reduction in computational cost while maintaining competitive performance. Similarly, DeepShift [11] introduces shift operations to replace multiplications, further improving computational efficiency by leveraging the simplicity of bitwise shifts. Both of these approaches have demonstrated that complex operations can be replaced by simpler alternatives without compromising accuracy, paving the way for more efficient deep learning models. Moreover, models like ShiftAddNet [12], which combine shift and addition operations, improve efficiency at the expense of increased parameter counts and limited

representational capacity. Specifically, the ShiftAddNet [12] architecture replaces convolutional layers with a combination of adder and shift layers, leading to a doubling of both the parameter count and the number of layers. Additionally, ShiftAddNet [12] freezes the weights of the shift layers, which can restrict the model’s learning potential and overall performance. These limitations highlight the need for a more balanced approach that can harness the benefits of both addition and shift operations without introducing such drawbacks.

While most of the work on operation-efficient neural networks has focused on CNNs for image processing, similar ideas can be applied to point cloud analysis models. Traditional approaches such as MLP-based architectures rely on shared MLP layers, which, despite their effectiveness, suffer from high computational costs due to their use of multiplication-heavy layers. The challenge lies in adapting the principles of addition and shift operations to MLPs, where the absence of convolutional operations requires different strategies for efficiency gains.

Building upon the insights from previous works, this study proposes a series of novel MLP-based architectures tailored for efficient point cloud classification. First, we introduce the Add-MLP model, which replaces the standard multiplication operations within MLP layers with addition operations based on the L_1 norm. By doing so, Add-MLP significantly reduces computational complexity while maintaining comparable performance to traditional MLPs. However, purely relying on additions, while computationally efficient, may limit the expressiveness of the model due to the inability to capture certain multiplicative transformations.

Next, the Shift-MLP model is introduced, which substitutes multiplication with bitwise shift operations. This approach leverages the minimal computational cost of shift operations, further enhancing the efficiency of the model. However, the expressiveness of shift operations is inherently limited to scaling by powers of two, which restricts the model’s ability to capture the full range of multiplicative mappings possible with floating-point multiplications. As a result, networks that rely solely on shift operations may struggle to approximate a broader range of transformations, limiting their overall performance in complex tasks.

The cornerstone of this study is the ShiftAdd-MLP (SA-MLP) architecture, which synergistically combines the strengths of both addition and shift operations. Unlike ShiftAddNet [12], which replaces convolutional layers and doubles the number of layers and parameters, SA-MLP focuses on replacing

MLP layers with alternately distributed adder and shift layers. This design maintains the original number of layers and avoids increasing the parameter count. By combining these operations, SA-MLP effectively addresses the limitations of the Add-MLP and Shift-MLP models. The adder layers contribute flexibility and fine-grained feature manipulation, while the shift layers offer coarse-grained efficiency and computational reduction. Furthermore, in contrast to the ShiftAddNet [12] model, where shift layer weights are frozen, SA-MLP allows for the learning of all parameters, thus preserving the model’s representational capacity .

A crucial innovation of SA-MLP is the application of different learning rates and optimizers for the adder and shift layers. This tailored optimization strategy ensures that each type of operation can contribute optimally to the learning process, enhancing the overall model performance without compromising efficiency. By decoupling the learning strategies for the adder and shift layers, SA-MLP fully exploits their complementary advantages, resulting in a model that offers both high accuracy and reduced computational overhead.

The main contributions of this study are as follows:

- We introduce Add-MLP and Shift-MLP, novel MLP-based architectures that replace multiplication operations with addition and shift operations, respectively, improving computational efficiency in point cloud classification tasks.
- We propose SA-MLP, which integrates adder and shift layers within MLPs, maintaining the original number of layers and parameters while ensuring full participation of all parameters in the learning process.
- We develop a tailored optimization strategy that applies distinct learning rates and optimizers for adder and shift layers, effectively leveraging their complementary strengths to enhance model performance.
- Extensive experimental evaluations demonstrate that the proposed SA-MLP outperforms the traditional multiplication-based MLP model and achieves comparable performance to state-of-the-art MLP-based models, offering a more efficient and scalable solution for point cloud classification.

2. Related works

2.1. Point Cloud Analysis

The burgeoning field of point cloud analysis has witnessed several innovative approaches leveraging deep learning to extract meaningful features from unstructured point sets. A pioneering work in this domain is the introduction of PointNet [7], which demonstrated the feasibility of directly processing point clouds with a deep learning framework. This was further expanded upon by PointNet++ [13], enhancing feature learning through a hierarchical structure that respects the metric space of point clouds. Convolutional Neural Networks (CNNs) have also been adapted to the point cloud domain, with PointCNN [14] standing out as a method that generalizes the convolution operation to point sets through a novel \mathcal{X} -Transformation. A parallel development in this space is the exploration of continuous convolutional neural networks [15], which aim to learn parametric filters for point cloud data. Graph Neural Networks (GNNs) have emerged as a powerful tool for point cloud analysis, with Dynamic Graph CNN [16] introducing a dynamic graph construction approach that adapts to the local geometry of point clouds. Building upon this, Adaptive Graph Convolution [8] has been proposed to further refine the feature extraction process through an adaptive scheme. In a significant departure from traditional convolutional and graph-based methods, Transformer architectures have made their mark in point cloud analysis with the advent of Point Transformer [17]. This approach utilizes the self-attention mechanism to capture global dependencies within point sets. Subsequent advancements have led to Point Transformer V2 [18], which introduces grouped vector attention and partition-based pooling to enhance the model’s capability.

2.2. Multiplication-Free Neural Networks

The pursuit of computational efficiency in deep learning has led to the emergence of Multiplication-Free neural networks, a paradigm shift aimed at reducing the computational complexity of convolutional operations. In this context, several approaches have been explored to construct neural networks without the need for multiplication, a conventionally resource-intensive operation.

Works such as BNN [19], XNOR-Net [20] and approach [21] have ventured into binarizing weights or activations, significantly curtailing the computational load by enabling operations to be performed using simple sign

determinations instead of floating-point multiplications. This approach not only streamlines the computational process but also compresses the model size, facilitating deployment on devices with limited resources. Shift operations, another avenue explored by SSL [22], Shift [23] and DeepShift [11], offer an alternative to multiplication by leveraging the hardware efficiency of bitwise operations. These operations, being inherently faster and less resource-demanding, provide a compelling solution for accelerating neural network implementations. The innovative approach of AdderNet [10] and subsequent works like AdderSR [24] and approach [25], which rely on additive operations, challenge the traditional reliance on multiplication in neural networks. By employing addition as the fundamental operation, these networks demonstrate that it is possible to achieve high performance with reduced computational overhead. Furthermore, the hybrid approach combining both shift and add operations, as seen in ShiftAddNet [12] and ShiftAddViT [26], has shown to be particularly effective. These models harness the strengths of both operations, offering a flexible trade-off between accuracy and efficiency.

In summary, while Multiplication-Free neural networks have made strides in efficiency, their application to point cloud analysis is relatively unexplored. This study breaks new ground by integrating shift and add operations into point cloud classification, demonstrating that these networks can achieve high accuracy with reduced computational costs.

3. Methodology

This section outlines the methodologies underpinning our efficient point cloud classification models. We begin with the conventional Multiplication MLP (Mul-MLP) as a baseline, then introduce the Add-MLP and Shift-MLP models, which respectively replace multiplications with additions and bitwise shifts to enhance computational efficiency. Advancing further, the ShiftAdd-MLP (SA-MLP) model harmoniously combines these operations, aiming to achieve a synergistic balance between efficiency and representational capacity. The section concludes with a discussion on the optimization strategies tailored for the proposed models, emphasizing the assignment of distinct learning rates and optimizers to different layer types to fully harness their individual advantages in enhancing classification accuracy and efficiency.

3.1. Baseline Model: Mul-MLP

Inspired by the use of shared MLPs in MLP-based models [7, 27], and the tokenization approach for obtaining local embeddings and complementary positional information in Vision Transformers (ViT) [28], this study proposes a baseline model named Multiplication MLP (Mul-MLP) for point cloud classification. The Mul-MLP model is designed with a concise structure that effectively captures the essential features of 3D point clouds while maintaining computational efficiency, illustrated in Fig 1.

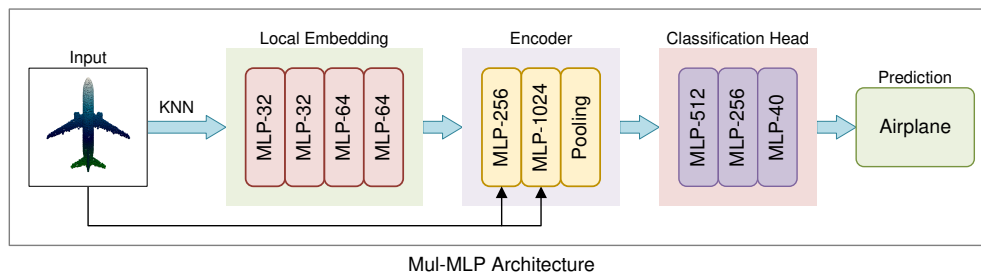


Figure 1: Architecture of the Multiplication-Based MLP (Mul-MLP) Model. This diagram illustrates the structure of the Mul-MLP model, where all layers utilize traditional multiplication operations for feature extraction and classification.

The Mul-MLP model consists of three primary components: a local embedding module, an encoder, and a classification header. Given an input point cloud $P \in \mathbb{R}^3$, the local embedding module first extracts local embedding features for each point. This is achieved by considering the local geometric context of each point, thereby capturing both the spatial relationships and the intrinsic properties of the point cloud. The extracted local embedding features are then passed into the encoder, which forms the core of the Mul-MLP model. Each layer of the encoder concatenates the input features with the corresponding global point coordinates before processing them. By integrating the local features with their spatial positions at every layer, the encoder ensures that both the detailed local geometry and the broader spatial distribution of points are effectively captured, allowing the model to maintain an awareness of the spatial arrangement throughout the network. The fusion of local and global information at each layer enhances the model’s ability to learn complex spatial patterns. After passing through the encoder, a global feature representation of the shape is obtained via max-

imum pooling across all points. This pooled feature, which represents the overall structure of the point cloud, is then fed into the classification header. The classification header consists of a series of fully connected layers that ultimately output the class prediction for the input point cloud.

The Mul-MLP model serves as a foundational baseline for this study, providing a benchmark against which the proposed variants, Add-MLP, Shift-MLP, and SA-MLP, are compared. By leveraging the simplicity and efficiency of MLPs, Mul-MLP sets a strong baseline in terms of both performance and computational cost for point cloud classification tasks.

3.2. Shift-Based Model: Shift-MLP

The Shift-MLP model proposed in this study introduces an innovative approach by replacing the traditional multiplication operations in MLP layers with bitwise shift operations, significantly improving computational efficiency without compromising model performance. The underlying principle of the shift layer involves quantizing the weights to powers of two, thereby transforming multiplication into efficient shift operations. In the forward propagation, each weight W is first quantized using the formulas $S = \text{sign}(W)$ and $p = \text{round}(\log_2(|W|))$, resulting in a quantized weight:

$$W_s = S \cdot 2^p \quad (1)$$

This quantization allows the model to compute the output as:

$$Y = W_s \cdot X \quad (2)$$

This approach effectively reduces the computational cost associated with floating-point multiplications. The network structure diagram for Shift-MLP is shown in Figure 2.

In the backpropagation process, the gradients are computed similarly to traditional MLPs, with minor adjustments due to the quantization step. The partial derivative of the loss L with respect to the input X is given by:

$$\frac{\partial L}{\partial X} = \frac{\partial L}{\partial Y} \cdot W_s \quad (3)$$

while the gradient with respect to the weight W is approximated as:

$$\frac{\partial L}{\partial W} \approx \frac{\partial L}{\partial Y} \cdot X \quad (4)$$

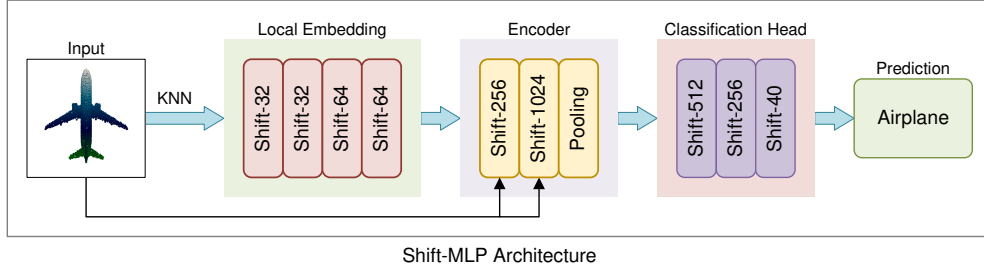


Figure 2: Architecture of the Shift-Based MLP (Shift-MLP) Model. This diagram shows the structure of the Shift-MLP model, where all layers employ bitwise shift operations to achieve computational efficiency.

assuming $\frac{\partial W_s}{\partial W} \approx 1$. This assumption simplifies the backpropagation, allowing the model to leverage the efficient forward computation without altering the training dynamics significantly. It’s important to note that during training, the quantization is only applied during the forward pass, leaving the backpropagation process consistent with traditional MLPs. This design choice ensures that the model benefits from the efficiency of shift operations while maintaining the learning capabilities of standard MLPs.

The Shift-MLP network, built using the described shift layers, demonstrates a balanced trade-off between computational efficiency and model accuracy. The model operates by converting the input into a 32-bit fixed-point representation, with 16 bits allocated for the integer part and 16 bits for the fractional part. The weights are stored in a compact 5-bit format, where 1 bit represents the sign S , and the remaining 4 bits store the shift amount p . To optimize the quantization process, the weights W are clamped to lie within the range of ± 1 before quantization, based on statistical analyses of traditional MLP networks, which have shown that most weights fall within this range after training. This clamping ensures that only left shifts are required, allowing the 4 bits to be used exclusively for storing the shift amount p , without needing to save the sign of the shift. By confining the weights within a small range close to zero, the quantization error is minimized, thereby maintaining high accuracy despite the reduced precision. This design consideration significantly enhances the model’s performance while preserving computational efficiency, making Shift-MLP a powerful approach for point cloud classification.

3.3. Addition-Based Model: Add-MLP

In this study, we propose Add-MLP, a MLP-based model designed for point cloud classification, as illustrated in Fig. 3. The Add-MLP model is inspired by the design principles of AdderNet [10], replacing traditional multiplication-based operations with addition to achieve greater computational efficiency without sacrificing model accuracy. Unlike conventional models that rely on dot products to compute activations, Add-MLP leverages the L_1 norm between the input features X and the weights W as a measure of relevance. This substitution provides a significant computational advantage, particularly in resource-constrained environments.

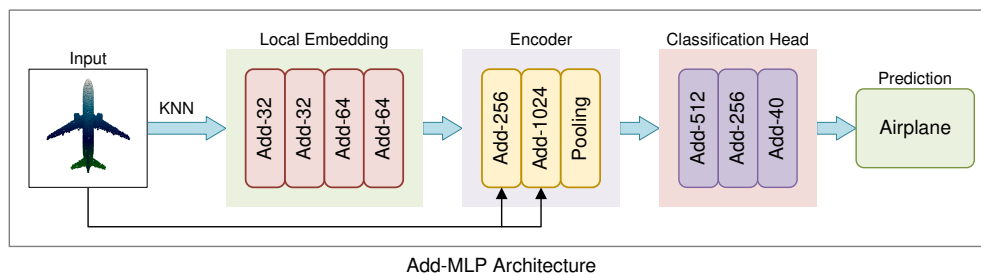


Figure 3: Architecture of the Addition-Based MLP (Add-MLP) Model. This diagram presents the structure of the Add-MLP model, which replaces traditional multiplication operations with adder layers throughout the network.

The forward propagation process in Add-MLP is governed by the following equation:

$$Y = - \| X - W \|_1 \quad (5)$$

where Y is the output, X is the input, and W represents the corresponding weights. The use of the L_1 norm allows the network to measure relevance based on additive differences, which fundamentally reduces the computational complexity compared to traditional multiplication-based operations.

The backward propagation process in Add-MLP introduces key adjustments to the gradient calculation. Initially, the gradient of the loss L with respect to the weights W is derived as:

$$\frac{\partial L}{\partial W} = \frac{\partial L}{\partial Y} \cdot \text{sign}(X - W) \quad (6)$$

This formulation reflects the nature of the L_1 norm, where the gradient is typically defined by the sign of the difference between X and W . However, in practice, this leads to challenges during training due to the discrete nature of the sign function, which can cause unstable weight updates and hinder convergence. To address this, the gradient is modified to:

$$\frac{\partial L}{\partial W} = \frac{\partial L}{\partial Y} \cdot (X - W) \quad (7)$$

This modification smooths the gradient, converting the coarse sign-based updates into more granular adjustments. The transition from $\text{sign}(X - W)$ to $X - W$ ensures that the gradient retains continuous information, facilitating more stable and effective learning.

Similarly, the gradient of the loss with respect to the input X is initially calculated as:

$$\frac{\partial L}{\partial X} = -\frac{\partial L}{\partial Y} \cdot \text{sign}(X - W) \quad (8)$$

and then modified to:

$$\frac{\partial L}{\partial X} = -\frac{\partial L}{\partial Y} \cdot (X - W) \quad (9)$$

This modification, like with the gradient for W , ensures a smooth and continuous gradient, which is essential for stable training. However, unlike the gradient for W , the gradient of X impacts all preceding layers due to the chain rule in backpropagation. This accumulation of gradients across multiple layers can lead to gradient explosion, causing instability in the model’s training. To mitigate this risk, a clipping function is applied:

$$\frac{\partial L}{\partial X} = -\frac{\partial L}{\partial Y} \cdot \text{clip}(X - W) \quad (10)$$

where:

$$\text{clip}(x) = \begin{cases} 1, & \text{if } x > 1, \\ x, & \text{if } -1 \leq x \leq 1, \\ -1, & \text{if } x < -1. \end{cases} \quad (11)$$

The clipping operation ensures that the gradient remains within a bounded range, thereby stabilizing the training process and preventing the runaway growth of gradients that could lead to numerical instability.

The Add-MLP network incorporates these adder layers to achieve a balance between computational efficiency and model performance. By shifting

from multiplication to addition and making thoughtful adjustments to the gradients, Add-MLP offers a robust and accurate approach to point cloud classification. These innovations ensure that the model remains stable during training, without sacrificing the quality of its predictions. Add-MLP exemplifies a novel approach to neural network design, showing that with thoughtful adjustments to core operations and gradient calculations, it is possible to achieve both high efficiency and robust performance. The adjustments to the gradients of both W and X are key to the network’s success, ensuring stability and effectiveness throughout the training process.

3.4. Combined Model: ShiftAdd-MLP (SA-MLP)

The SA-MLP model introduced in this study builds on the concepts of Shift-MLP and Add-MLP, offering an advanced approach that fully leverages the complementary strengths of shift and add operations (see Fig. 4). Unlike ShiftAddNet [12], which operates in the image domain and doubles the number of layers by replacing each convolutional layer with a pair of Shift and Adder layers, SA-MLP integrates these operations in an interleaved manner within the MLP framework. The key innovation lies in replacing the traditional MLP layers in the baseline Mul-MLP model with a sequence of interleaved Shift and Adder layers. This design ensures that the number of layers and parameters remains consistent with the original model, avoiding the significant increase in complexity observed in ShiftAddNet [12].

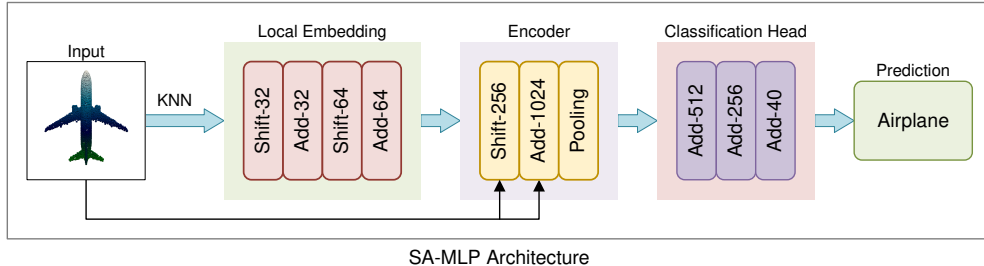


Figure 4: Architecture of the ShiftAdd-MLP (SA-MLP) Model. This diagram depicts the structure of the SA-MLP model, integrating both adder and shift layers to leverage the complementary strengths of each operation.

A critical distinction between SA-MLP and ShiftAddNet [12] lies in the treatment and optimization of the shift and adder layers. In ShiftAddNet [12],

the shift layer is frozen during training, preventing it from contributing to learning and reducing it to a source of random perturbation, which can degrade overall network performance. In contrast, SA-MLP allows both shift and adder layers to actively participate in the learning process by using differentiated optimization strategies tailored to the characteristics of each layer type. Although these strategies are only briefly mentioned here, they are vital to SA-MLP’s superior performance and will be detailed in the following subsection (Sec. 3.5), which discusses the optimization techniques for Shift-MLP, Add-MLP, and SA-MLP.

The motivation for combining shift and add operations in SA-MLP stems from the unique yet complementary strengths of each. Shift operations are highly efficient, reducing computational overhead through bitwise shifts, while add operations enhance feature extraction by enabling richer non-linear transformations. By interleaving these operations, SA-MLP captures a wide range of features with minimal parameter overhead, achieving an optimal balance between computational cost and performance, which is particularly advantageous in resource-constrained environments.

The SA-MLP network structure demonstrates how interleaved shift and adder layers systematically replace the traditional MLP layers. This design maintains the depth and parameter count of the original Mul-MLP model while improving its ability to extract and process features from point cloud data. The careful integration of these operations within the network allows SA-MLP to achieve high computational efficiency and model accuracy, making it an effective solution for point cloud analysis tasks where both performance and resource efficiency are critical.

3.5. Optimization Strategies for Shift and Adder Layers in SA-MLP

To address the distinct characteristics of the shift and adder layers in the SA-MLP model, this subsection elaborates on the necessity of individualized optimization strategies for each type. The shift layer, being structurally similar to the traditional multiplication-based MLP, requires minimal adjustments in optimization. In contrast, the adder layer, which fundamentally diverges from conventional operations, demands a more nuanced approach to ensure effective parameter updates.

3.5.1. Shift Layer Optimization

The shift layer replaces traditional multiplication with shift operations, incorporating quantization of weights to powers of two. Despite this modifica-

tion, the forward and backward propagation processes remain closely aligned with those of the traditional multiplication-based MLP model. Consequently, the gradients and weight distributions do not significantly deviate, allowing for the adoption of standard optimization strategies. This study applies a cyclical learning rate schedule, coupled with the Adam optimizer, which has proven effective for similar architectures.

3.5.2. Adder Layer Optimization

The adder layer, on the other hand, introduces a substantial deviation from conventional architectures. It computes the correlation between input X and weight W using the negative L_1 norm, $-\|X - W\|_1$, which results in negative outputs that approach zero as the correlation strengthens. This contrasts sharply with traditional MLPs and CNNs, where stronger correlations yield higher, unbounded activation values. This fundamental difference leads to distinct output distributions and a significant divergence in gradient behavior between the adder and shift layers.

The gradient calculation for the adder layer incorporates the factor $(X - W)$, and at high activation values, this term approaches zero, causing a sharp decline in gradient magnitude. This can result in ineffective updates if the same optimization strategy as the shift layer is applied. Additionally, the consistent subtraction of X and W necessitates that their magnitudes are aligned. Given that input X often undergoes batch normalization, it is crucial to normalize the gradient of W to maintain effective learning.

To address these challenges, this study employs a gradient modulation strategy inspired by AdderNet [10]. The gradient modulation is represented by the following formula:

$$\tilde{g} = \frac{\eta \nabla L(W)}{\|\nabla L(W)\|_2 / \sqrt{n}} \quad (12)$$

where \tilde{g} is the modulated gradient, η is a hyperparameter that adjusts the gradient magnitude, n is the number of elements in W , and $\nabla L(W)$ is the gradient of the loss L with respect to W .

The update to weight W is then calculated as:

$$\Delta W = l \times \tilde{g} \quad (13)$$

where ΔW represents the update amount, and l is the learning rate. Additionally, because Adam’s adaptive gradient adjustments might conflict with

the gradient modulation strategy, the SGD optimizer is chosen for the adder layer. This choice ensures compatibility with the gradient adjustment mechanism and improves update accuracy.

3.5.3. Integrated Optimization in SA-MLP

The distinction between the shift and adder layers necessitates carefully designed optimization strategies to ensure the overall performance of the SA-MLP model. While ShiftAddNet [12] previously opted to freeze the shift layer to maintain optimization stability, this approach compromises the model’s adaptability. By contrast, this study’s individualized optimization for each layer type allows the SA-MLP to fully leverage the complementary strengths of both the shift and adder operations. The integration of shift and add operations in SA-MLP combines the computational efficiency of shifts with the enhanced feature extraction capabilities of additions. This hybrid approach strikes a balance between computational cost and model performance, making SA-MLP particularly suitable for scenarios where both efficiency and accuracy are crucial.

4. Experiments

This section begins by detailing the parameter configurations, followed by a presentation of the experimental results for point cloud classification. Finally, to provide deeper insights into the design rationale behind the SA-MLP model, we include visualizations and statistical analyses.

4.1. Training Configuration

To ensure a fair comparison across all models, this study utilizes a uniform framework and consistent training parameters. The evaluation is conducted on the point cloud classification task using the ModelNet40 benchmark, which comprises 12,311 samples across 40 categories, with 9,843 samples for training and 2,468 for testing. Each point cloud input contains 1,024 points. A periodic annealing learning rate is employed with a batch size of 32 for all models. For Mul-MLP and Shift-MLP, the learning rate starts at 10^{-3} and is reduced to 10^{-6} , with the Adam optimizer used for training. Conversely, Add-MLP employs a higher initial learning rate of 2×10^{-2} that decreases to 2×10^{-3} and utilizes the SGD optimizer. The SA-MLP model integrates a hybrid optimization strategy: the shift layers follow the same parameters as Shift-MLP, while the adder layers adopt the approach used

in Add-MLP. This setup allows each model to be trained under consistent conditions while accounting for their unique optimization requirements.

4.2. Classification Task

In this subsection, we evaluate the performance of the SA-MLP model proposed in this study against several state-of-the-art methods on the ModelNet40 classification task. The results of this comparative analysis are summarized in Tab. 1.

Method	Input	Num.	Acc. (%)
PointNet [7]	xyz	1k	89.2
PointNet++(MSG) [13]	xyz, nor	5k	91.9
PointCNN [14]	xyz	1k	92.2
DGCNN [16]	xyz	1k	92.9
KPConv [29]	xyz	6.8k	92.9
PointNext [30]	xyz	1k	93.2
AdaptConv [31]	xyz	1k	93.4
PointMixer [32]	xyz	1k	93.6
PT [17]	xyz	1k	93.7
Mul-MLP	xyz	1k	93.5
Shift-MLP	xyz	1k	93.3
Add-MLP	xyz	1k	93.1
SA-MLP	xyz	1k	93.9

Table 1: Results for the ModelNet40 classification task.

Tab. 1 illustrates the performance of various MLP-based methods, including PointNet [7], PointNet++[13], and PointNext[30]. Remarkably, the SA-MLP model proposed in this study surpasses these established methods, achieving a classification accuracy of 93.9%. This notable improvement underscores the efficacy of combining both shift and add operations within the MLP framework, as demonstrated in this research. The inclusion of these operations enhances the model’s ability to extract and process point cloud features, contributing to its superior performance.

In addition to benchmarking SA-MLP against external methods, the study also evaluates the performance of four models developed as part of this research: Mul-MLP, Shift-MLP, Add-MLP, and SA-MLP. Mul-MLP serves as the baseline model, achieving an accuracy of 93.5%, which establishes

a strong foundation for comparison. Shift-MLP and Add-MLP, which replace multiplication operations with shift and add operations, respectively, achieve slightly lower accuracies of 93.3% and 93.1%. While both models demonstrate competitive performance and offer substantial improvements in computational efficiency, their slight reduction in accuracy reflects the trade-off typically encountered when replacing multiplication operations with more efficient alternatives.

However, the hybrid SA-MLP model, which synergistically integrates both shift and add operations, significantly outperforms the baseline, achieving an accuracy of 93.9%. This result demonstrates the complementary strengths of the two operations—shift operations contribute to efficient computation, while add operations enhance the model’s ability to capture complex feature representations. The interleaving of these two operations enables SA-MLP to strike a balance between efficiency and accuracy, making it particularly suitable for resource-constrained environments where computational cost is a critical factor.

This comparative analysis highlights the promising potential of developing multiplication-free architectures for point cloud analysis. While both Shift-MLP and Add-MLP deliver increased efficiency, it is the hybrid design of SA-MLP that capitalizes on their combined advantages, resulting in a significant performance gain. The results of this study pave the way for future research into the development of more efficient and effective point cloud analysis models, offering an innovative solution for real-time and resource-constrained applications.

4.3. Performance Across Point Cloud Densities

The table 2 presents the classification accuracy of four models—Mul-MLP, Shift-MLP, Add-MLP, and SA-MLP—on the ModelNet40 dataset, evaluated with varying point cloud densities: 1024, 512, 256, and 128 points. Across all models, there is a clear trend: as the number of points decreases, the classification accuracy generally declines. This pattern is expected, as a lower number of points reduces the amount of information available for feature extraction, making it more challenging for the models to accurately classify the point clouds. However, the extent of this decline varies among the models, providing insight into their robustness to changes in point cloud density.

The comparative analysis of the first three models—Mul-MLP, Shift-MLP, and Add-MLP—reveals a consistent order of accuracy across different

Model	1024	512	256	128
Mul-MLP	93.5	92.9	92.7	90.5
Shift-MLP	93.3	92.7	91.7	89.1
Add-MLP	93.1	92.6	90.2	87.0
SA-MLP	93.9	93.1	91.7	90.0

Table 2: Classification accuracy of Mul-MLP, Shift-MLP, Add-MLP, and SA-MLP models on ModelNet40 across varying point cloud densities.

point densities, with Mul-MLP performing the best, followed by Shift-MLP, and then Add-MLP. This trend underscores the inherent differences in the operations that underpin each model. Mul-MLP, which relies on traditional multiplication operations, provides the most stable and accurate performance across all densities due to its fine-grained feature extraction capabilities. Shift-MLP, though slightly less accurate than Mul-MLP, remains close in performance, leveraging the efficiency of bitwise shift operations. However, the slight drop in accuracy for Shift-MLP indicates that while shift operations are computationally efficient, they may lack the precision needed for capturing detailed features as effectively as multiplication-based operations.

Add-MLP exhibits the most significant performance degradation as the point cloud density decreases. This decline is particularly pronounced at lower densities (256 and 128 points), where the model’s accuracy drops more sharply compared to Mul-MLP and Shift-MLP. The sensitivity of Add-MLP to reduced point cloud density can be attributed to the nature of the adder layer, which relies on the L_1 norm to measure the relevance between input features and weights. The L_1 norm’s strict requirement for matching weights and features makes Add-MLP more susceptible to noise and data sparsity, leading to less effective feature extraction when fewer points are available. As the point cloud becomes sparser, the model struggles to maintain high accuracy, reflecting the limitations of additive operations in handling lower-density data.

The SA-MLP model, which integrates both shift and add operations, demonstrates a significant performance advantage over the baseline Mul-MLP model at higher point densities (1024 and 512 points). This improvement highlights the benefits of combining the complementary strengths of shift and add operations, allowing SA-MLP to better capture a broader range of features with minimal parameter overhead. However, as the point density

decreases, the performance of SA-MLP shows a slight decline compared to Mul-MLP, particularly at the lowest density of 128 points. This decrease is primarily due to the inclusion of the adder layer, which, as discussed earlier, is more sensitive to noise and data sparsity. Despite this, SA-MLP maintains competitive performance, demonstrating that the hybrid approach offers a balanced trade-off between computational efficiency and accuracy, even under challenging conditions.

When comparing SA-MLP with Shift-MLP and Add-MLP, SA-MLP consistently outperforms both across all point densities. The hybrid nature of SA-MLP enables it to leverage the advantages of both shift and add operations, making it more robust and adaptable to varying input conditions. The shift layers contribute to maintaining high computational efficiency, while the add layers enhance the model’s ability to capture complex feature interactions. This combination allows SA-MLP to achieve superior accuracy and resilience, making it a particularly effective model for point cloud classification tasks where both performance and resource efficiency are crucial.

In summary, the experimental results underscore the effectiveness of the SA-MLP model in combining shift and add operations to create a robust and efficient architecture for point cloud classification. While each type of operation has its strengths and weaknesses, the hybrid approach of SA-MLP allows it to maintain high performance across different input densities, making it a promising direction for future research in the development of advanced neural network models.

4.4. Analysis of Gradient Regularization Across Layer Types

This subsection analyzes the gradient regularization applied across different layer types, specifically focusing on the adder layers compared to multiplication-based and shift-based layers. The analysis examines the root-mean-square (RMS) values of the gradients across various embedding and encoder layers, as shown in Tab. 3. The table categorizes the different layers based on their operational types: multiplication (mul.), shift, and addition (add), with special consideration for the adder layers’ vanilla gradients before adaptive modulation (add (van.)).

The results reveal that the RMS values of the gradients for both the shift layers in Shift-MLP and SA-MLP, as well as the multiplication-based layers in Mul-MLP, are consistently of the same order of magnitude. This consistency suggests that shift operations can effectively replace multiplication operations

Model	type	Embedding Layers				Encoder Layers	
		<i>l</i> -1	<i>l</i> -2	<i>l</i> -3	<i>l</i> -4	<i>l</i> -1	<i>l</i> -2
Mul-MLP	mul. ($\times 10^{-5}$)	21.6	7.88	4.79	3.73	8.77	2.58
Shift-MLP	shift ($\times 10^{-5}$)	2.49	3.30	1.36	1.85	4.43	1.14
Add-MLP	add (van.) ($\times 10^{-5}$)	8.93	1.25	0.35	0.30	0.20	0.06
	add ($\times 1.0$)	0.20	0.20	0.20	0.20	0.20	0.20
SA-MLP	shift ($\times 10^{-5}$)	14.4	-	9.56	-	4.84	-
	add (van.) ($\times 10^{-5}$)	-	1.03	-	0.91	-	0.07
	add ($\times 1.0$)	-	0.20	-	0.20	-	0.20

Table 3: Comparison of Root-Mean-Square (RMS) values of gradients across embedding and encoder layers for Mul-MLP, Shift-MLP, Add-MLP, and SA-MLP models.

without significantly altering the gradient magnitude, which is critical for maintaining stable training dynamics across these models.

However, the RMS values for the raw gradients of the adder layers in Add-MLP and SA-MLP are significantly lower and vary more across layers, particularly as the network depth increases. This variability in gradient magnitude complicates the optimization process, making it challenging to apply a uniform learning rate across the network. The differences in gradient magnitude between layers within the adder layers further emphasize the need for a more tailored approach to gradient management.

To address this issue, an adaptive modulation technique is applied to the adder layer gradients, ensuring that the RMS values after regularization are consistently set at 0.2 across all adder layers. This outcome is derived from the expression for the regularized gradient \tilde{g} outlined in the Methodology section (Eq. 12). The RMS of the regularized gradient, \tilde{g}_{rms} , is calculated

as follows:

$$\tilde{g}_{rms} = \frac{\eta}{\|\nabla L(W)\|_2 / \sqrt{n}} \times \frac{\|\nabla L(W)\|_2}{\sqrt{n}} = \eta \quad (14)$$

Here, η is set to 0.2, effectively representing the variance of the adder layer gradient after adaptive modulation. This regularization standardizes the gradient variance across all adder layers, facilitating the use of a uniform learning rate. However, it is important to note that even after modulation, the magnitude of the gradients in the adder layers remains very different from that of the multiplication and shift layers, necessitating distinct optimization strategies. Specifically, the choice of optimizer for the adder layers diverges from that used for the multiplication and shift layers. While Adam is typically used for its adaptive gradient adjustment, this could conflict with the already stabilized gradients in the adder layers. Therefore, a simpler optimizer, such as SGD, is chosen to avoid introducing further unnecessary modulation.

In summary, the regularization of the adder layer gradients plays a crucial role in maintaining training stability and enabling effective optimization. The necessity for distinct learning rates and optimizers for the different layer types highlights the inherent differences in their operational characteristics, ensuring that the SA-MLP model can leverage the strengths of each layer type while maintaining overall performance stability.

4.5. Visualization Analysis of Encoder Features

To further analyze the feature representations learned by each model, we applied t-distributed Stochastic Neighbor Embedding (t-SNE) visualization to the encoded features from the test set. The resulting plots are shown in Fig. 5. The feature distribution in Fig. 5 (a) represents the baseline Mul-MLP model, which serves as the reference for comparison. Fig. 5 (a) displays a generally well-separated clustering of samples, indicating that Mul-MLP effectively captures the underlying structure of the data.

In Fig. 5 (b), which corresponds to the Shift-MLP model, the distribution is largely similar to that of the baseline Mul-MLP. This similarity suggests that replacing multiplication with shift operations does not significantly alter the model’s ability to distinguish between categories, while still offering the computational benefits of the shift operation. The clusters remain well-defined, and there is minimal overlap between different categories, indicating that Shift-MLP retains a robust feature extraction capability.

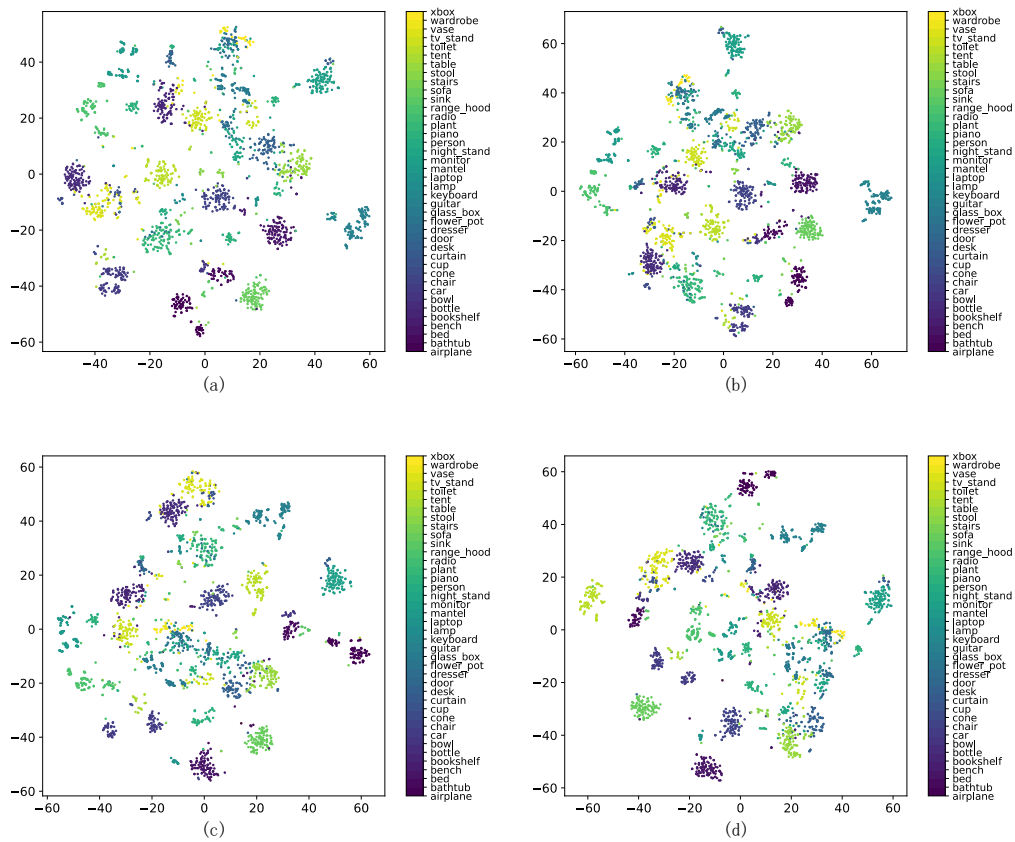


Figure 5: t-SNE visualization of the coded features from the test set for each model: (a) Mul-MLP (baseline), (b) Shift-MLP, (c) Add-MLP, and (d) SA-MLP. The visualizations highlight the feature distributions and clustering behavior of the models, with SA-MLP demonstrating tighter clustering and fewer outliers.

Fig. 5 (c), representing the Add-MLP model, shows some notable differences compared to the baseline. Specifically, there is an increase in overlap between categories in certain regions of the plot. This suggests that the adder layers, which rely on additive operations, may introduce some challenges in distinguishing between closely related categories. The increased repetition between categories could be due to the sensitivity of the L_1 norm to noise and the reduced capability of additive operations to capture complex feature relationships as effectively as multiplication.

The most significant observations arise from Fig. 5 (d), which corresponds to the SA-MLP model. Compared to the baseline, SA-MLP shows tighter clustering within categories and fewer discrete points or outliers. This improved clustering suggests that the integration of both shift and add operations enables SA-MLP to better capture the intrinsic structures of the data, leading to more compact and distinct feature representations. The fewer outliers indicate that SA-MLP may also be more resilient to variations within the data, resulting in more consistent classifications.

4.6. Weight Distribution Analysis Across Different Layer Types

In this subsection, we analyze the weight distributions of different layers across four models: Mul-MLP, Shift-MLP, Add-MLP, and SA-MLP. The analysis is conducted using statistical histograms that visualize the characteristics of the weight distributions for the two encoder layers in each model, illustrated in Fig. 6. Understanding these distributions provides insight into the underlying behavior of each model and highlights the differences between multiplication, shift, and add operations in neural networks.

In Mul-MLP, which utilizes traditional multiplication-based operations, the weight distributions for both encoder layers follow a Gaussian pattern. This pattern arises because the shared MLP weights in Mul-MLP are, under certain specific assumptions, equivalent to the L_2 norm, as supported by the literature [10]. This equivalence means that the optimization process, which minimizes the L_2 loss, naturally drives the weights toward a distribution centered around zero, resulting in the observed Gaussian pattern.

In contrast, Shift-MLP replaces the multiplication operations with bit-wise shift operations, and as a result, the weight distribution takes on a discrete form. This is due to the quantization process inherent in shift operations, where weights are quantized to specific powers of two. The histogram for Shift-MLP reveals several discrete columns, each corresponding to a quantized value. Despite this discretization, the overall envelope of the

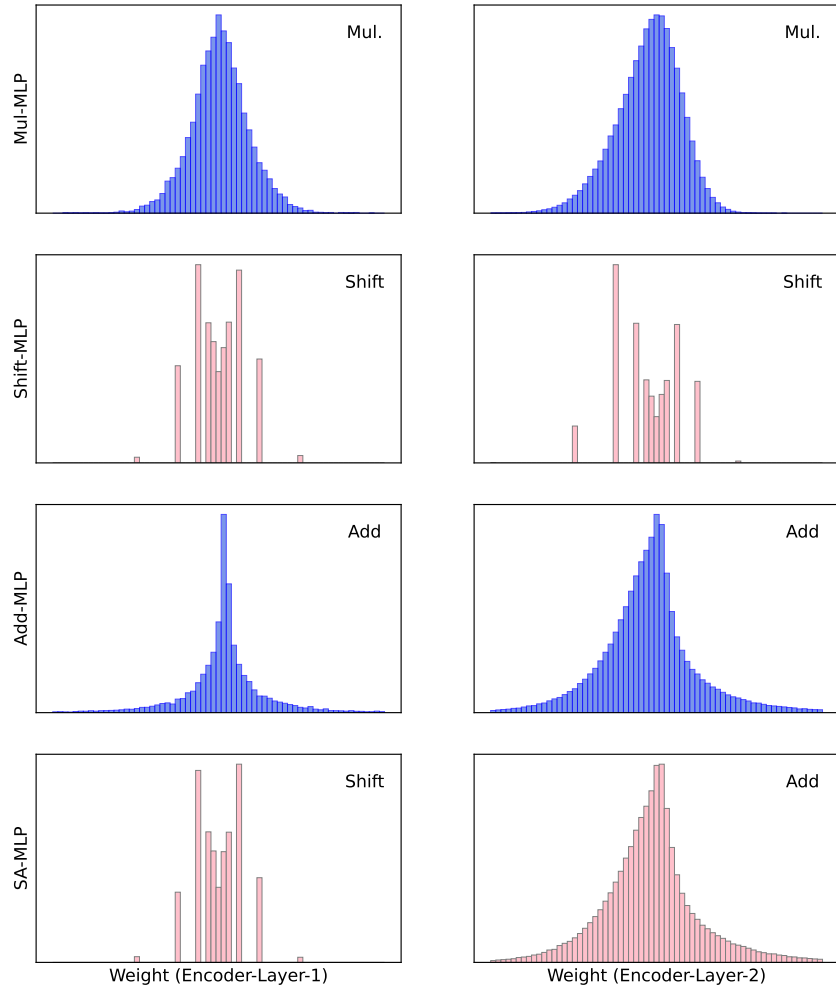


Figure 6: Histograms of weight distributions for different models and layers: (a) Mul-MLP, (b) Shift-MLP, (c) Add-MLP, and (d) SA-MLP. Each row represents a different model, while columns correspond to encoder layers. The histograms illustrate the distribution characteristics of weights across various layer types, showing differences in distribution patterns between multiplication-based, shift-based, and add-based layers.

distribution closely resembles the normal distribution observed in Mul-MLP, indicating that while the quantization introduces discrete characteristics, the general distribution pattern remains somewhat similar.

The Add-MLP model, which replaces multiplication with addition operations, shows a different pattern. The weights in Add-MLP exhibit a Laplace distribution, characterized by a sharper peak at the center and heavier tails compared to the normal distribution. This difference arises from the L_1 norm used in the adder layers, which penalizes large weight values more heavily than the L_2 norm. As a result, the optimization process in Add-MLP drives more weights to be close to zero, leading to the observed Laplace distribution. This pattern is consistent with findings in the AdderNet [10], where the L_1 paradigm was shown to produce such distributions due to the nature of the loss function driving weights to minimize the absolute differences rather than squared differences.

Finally, the SA-MLP model, which integrates both shift and add operations, exhibits a combination of these distribution patterns. The first encoder layer in SA-MLP is a shift layer, and its weight distribution mirrors that of Shift-MLP, with discrete quantized values forming the histogram. The second encoder layer is an adder layer, and its weight distribution aligns with that of Add-MLP, showing a Laplace distribution. This combination within SA-MLP highlights the complementary strengths of both shift and add operations, as the model can leverage the efficiency of quantized shifts in the earlier layers and the fine-tuned adjustments of the adder layers in subsequent layers.

5. Conclusion

This study proposed a series of multiplication-free MLP-based models targeted at improving the computational efficiency of point cloud classification tasks by replacing traditional multiplication operations with shift and add operations. Through extensive experimentation, we demonstrated that while individual models like Shift-MLP and Add-MLP offered comparable accuracy to multiplication-based models, the hybrid SA-MLP model, which strategically integrates both shift and add operations, emerged as the best performer. It not only outperformed the baseline Mul-MLP but also surpassed several state-of-the-art methods on the ModelNet40 classification benchmark, affirming the potential of multiplication-free architectures in high-accuracy, resource-efficient deep learning applications.

However, despite the promising results, the study also encountered significant limitations that warrant discussion. The training of the adder layer was notably slower compared to traditional multiplication-based models. This slowdown can be attributed to the current limitations in deep learning infrastructure, particularly with regard to the lack of optimization for non-standard operations like addition-based networks. Modern deep learning libraries, such as CUDA and CuDNN, have been extensively optimized for traditional convolutional operations through dedicated hardware acceleration, advanced algorithms, and auto-tuning capabilities, which significantly boost the performance of CNNs. In contrast, the addition and absolute value operations central to adder layers do not benefit from these optimizations, leading to inefficiencies during both forward inference and backpropagation. Although CUDA programming was employed in this study to optimize these operations, the results indicate that the training and inference speeds on GPU platforms are still inferior to those of traditional matrix multiplication-based models.

These limitations highlight the challenges of generalizing addition-based networks to more complex point cloud analysis tasks, such as semantic segmentation. While the SA-MLP model presents a viable solution for point cloud classification, its broader applicability remains constrained by the current state of deep learning infrastructure. Future research should explore the development of more optimized frameworks and hardware support for non-standard operations, which could unlock the full potential of addition-based networks. Moreover, investigating alternative strategies to mitigate the computational overhead of adder layers could pave the way for their integration into more complex and computationally intensive tasks. Despite these challenges, this study provides a foundation for further exploration into efficient, multiplication-free neural network architectures, with the potential to significantly impact the field of deep learning in resource-constrained environments.

References

- [1] E. E. Aksoy, S. Baci, S. Cavdar, Salsanet: Fast road and vehicle segmentation in lidar point clouds for autonomous driving, in: 2020 IEEE Intelligent Vehicles Symposium (IV), 2020, pp. 926–932. doi: 10.1109/IV47402.2020.9304694.

- [2] Y. Li, L. Ma, Z. Zhong, F. Liu, M. A. Chapman, D. Cao, J. Li, Deep learning for lidar point clouds in autonomous driving: A review, *IEEE Transactions on Neural Networks and Learning Systems* 32 (8) (2021) 3412–3432. doi:10.1109/TNNLS.2020.3015992.
- [3] L. Yang, Y. Liu, J. Peng, Z. Liang, A novel system for off-line 3d seam extraction and path planning based on point cloud segmentation for arc welding robot, *Robotics and Computer-Integrated Manufacturing* 64 (2020) 101929. doi:https://doi.org/10.1016/j.rcim.2019.101929.
- [4] J. Wiederer, A. Bouazizi, U. Kressel, V. Belagiannis, Traffic control gesture recognition for autonomous vehicles, in: *2020 IEEE/RSJ International Conference on Intelligent Robots and Systems (IROS)*, 2020, pp. 10676–10683. doi:10.1109/IROS45743.2020.9341214.
- [5] G. Bui, B. Morago, T. Le, K. Karsch, Z. Lu, Y. Duan, Integrating videos with lidar scans for virtual reality, in: *2016 IEEE Virtual Reality (VR)*, 2016, pp. 161–162. doi:10.1109/VR.2016.7504703.
- [6] S. Manivasagam, I. A. Bârsan, J. Wang, Z. Yang, R. Urtasun, Towards zero domain gap: A comprehensive study of realistic lidar simulation for autonomy testing, in: *2023 IEEE/CVF International Conference on Computer Vision (ICCV)*, 2023, pp. 8238–8248. doi:10.1109/ICCV51070.2023.00760.
- [7] R. Q. Charles, H. Su, M. Kaichun, L. J. Guibas, Pointnet: Deep learning on point sets for 3d classification and segmentation, in: *2017 IEEE Conference on Computer Vision and Pattern Recognition (CVPR)*, 2017, pp. 77–85. doi:10.1109/CVPR.2017.16.
- [8] M. Xu, R. Ding, H. Zhao, X. Qi, Paconv: Position adaptive convolution with dynamic kernel assembling on point clouds, in: *2021 IEEE/CVF Conference on Computer Vision and Pattern Recognition (CVPR)*, 2021, pp. 3172–3181. doi:10.1109/CVPR46437.2021.00319.
- [9] X.-F. Han, Y.-F. Jin, H.-X. Cheng, G.-Q. Xiao, Dual transformer for point cloud analysis, *IEEE Transactions on Multimedia* 25 (2023) 5638–5648. doi:10.1109/TMM.2022.3198318.
- [10] H. Chen, Y. Wang, C. Xu, B. Shi, C. Xu, Q. Tian, C. Xu, Addernet: Do we really need multiplications in deep learning?, in: *2020 IEEE/CVF*

- Conference on Computer Vision and Pattern Recognition (CVPR), 2020, pp. 1465–1474. doi:10.1109/CVPR42600.2020.00154.
- [11] M. Elhoushi, Z. Chen, F. Shafiq, Y. H. Tian, J. Y. Li, Deepshift: Towards multiplication-less neural networks, in: Proceedings of the IEEE/CVF Conference on Computer Vision and Pattern Recognition (CVPR) Workshops, 2021, pp. 2359–2368.
- [12] H. You, X. Chen, Y. Zhang, C. Li, S. Li, Z. Liu, Z. Wang, Y. Lin, Shiftaddnet: A hardware-inspired deep network, in: H. Larochelle, M. Ranzato, R. Hadsell, M. Balcan, H. Lin (Eds.), Advances in Neural Information Processing Systems, Vol. 33, Curran Associates, Inc., 2020, pp. 2771–2783.
URL https://proceedings.neurips.cc/paper_files/paper/2020/file/1cf44d7975e6c86cffa70cae95b5fbb2-Paper.pdf
- [13] C. R. Qi, L. Yi, H. Su, L. J. Guibas, Pointnet++: Deep hierarchical feature learning on point sets in a metric space, in: Advances in Neural Information Processing Systems, Vol. 30, 2017.
- [14] Y. Li, R. Bu, M. Sun, W. Wu, X. Di, B. Chen, Pointcnn: Convolution on x-transformed points, in: Proceedings of the 32nd International Conference on Neural Information Processing Systems, NIPS’18, Curran Associates Inc., Red Hook, NY, USA, 2018, p. 828–838.
- [15] S. Wang, S. Suo, W.-C. Ma, A. Pokrovsky, R. Urtasun, Deep parametric continuous convolutional neural networks, in: 2018 IEEE/CVF Conference on Computer Vision and Pattern Recognition (CVPR), 2018, pp. 2589–2597.
- [16] Y. Wang, Y. Sun, Z. Liu, S. E. Sarma, M. M. Bronstein, J. M. Solomon, Dynamic graph cnn for learning on point clouds, ACM Trans. Graph. 38 (5) (2019).
- [17] H. Zhao, L. Jiang, J. Jia, P. Torr, V. Koltun, Point transformer, in: 2021 IEEE/CVF International Conference on Computer Vision (ICCV), 2021, pp. 16239–16248. doi:10.1109/ICCV48922.2021.01595.
- [18] X. Wu, Y. Lao, L. Jiang, X. Liu, H. Zhao, Point transformer v2: Grouped vector attention and partition-based pooling, in: S. Koyejo,

- S. Mohamed, A. Agarwal, D. Belgrave, K. Cho, A. Oh (Eds.), *Advances in Neural Information Processing Systems*, Vol. 35, 2022, pp. 33330–33342.
- [19] I. Hubara, M. Courbariaux, D. Soudry, R. El-Yaniv, Y. Bengio, Binarized neural networks, in: D. Lee, M. Sugiyama, U. Luxburg, I. Guyon, R. Garnett (Eds.), *Advances in Neural Information Processing Systems*, Vol. 29, Curran Associates, Inc., 2016.
URL https://proceedings.neurips.cc/paper_files/paper/2016/file/d8330f857a17c53d217014ee776bfd50-Paper.pdf
- [20] M. Rastegari, V. Ordonez, J. Redmon, A. Farhadi, Xnor-net: Imagenet classification using binary convolutional neural networks, in: B. Leibe, J. Matas, N. Sebe, M. Welling (Eds.), *Computer Vision – ECCV 2016*, Springer International Publishing, Cham, 2016, pp. 525–542.
- [21] Z. Lin, M. Courbariaux, R. Memisevic, Y. Bengio, Neural networks with few multiplications (2016). [arXiv:1510.03009](https://arxiv.org/abs/1510.03009).
URL <https://arxiv.org/abs/1510.03009>
- [22] W. Chen, D. Xie, Y. Zhang, S. Pu, All you need is a few shifts: Designing efficient convolutional neural networks for image classification, in: *2019 IEEE/CVF Conference on Computer Vision and Pattern Recognition (CVPR)*, 2019, pp. 7234–7243. doi:10.1109/CVPR.2019.00741.
- [23] B. Wu, A. Wan, X. Yue, P. Jin, S. Zhao, N. Golmant, A. Gholaminejad, J. Gonzalez, K. Keutzer, Shift: A zero flop, zero parameter alternative to spatial convolutions, in: *2018 IEEE/CVF Conference on Computer Vision and Pattern Recognition*, 2018, pp. 9127–9135. doi:10.1109/CVPR.2018.00951.
- [24] D. Song, Y. Wang, H. Chen, C. Xu, C. Xu, D. Tao, Addersr: Towards energy efficient image super-resolution, in: *2021 IEEE/CVF Conference on Computer Vision and Pattern Recognition (CVPR)*, 2021, pp. 15643–15652. doi:10.1109/CVPR46437.2021.01539.
- [25] Y. Wang, M. Huang, K. Han, H. Chen, W. Zhang, C. Xu, D. Tao, Addernet and its minimalist hardware design for energy-efficient artificial intelligence (2021). [arXiv:2101.10015](https://arxiv.org/abs/2101.10015).
URL <https://arxiv.org/abs/2101.10015>

- [26] H. You, H. Shi, Y. Guo, Y. Lin, Shiftaddvit: Mixture of multiplication primitives towards efficient vision transformer, in: A. Oh, T. Naumann, A. Globerson, K. Saenko, M. Hardt, S. Levine (Eds.), *Advances in Neural Information Processing Systems*, Vol. 36, Curran Associates, Inc., 2023, pp. 33319–33337.
URL https://proceedings.neurips.cc/paper_files/paper/2023/file/69c49f75ca31620f1f0d38093d9f3d9b-Paper-Conference.pdf
- [27] Q. Zheng, J. Sun, W. Chen, A lightweight network for point cloud analysis via the fusion of local features and distribution characteristics, *Sensors* 22 (13) (2022). doi:10.3390/s22134742.
- [28] A. Dosovitskiy, L. Beyer, A. Kolesnikov, D. Weissenborn, X. Zhai, T. Unterthiner, M. Dehghani, M. Minderer, G. Heigold, S. Gelly, J. Uszkoreit, N. Houlsby, An image is worth 16x16 words: Transformers for image recognition at scale, in: *International Conference on Learning Representations*, 2021.
- [29] H. Thomas, C. R. Qi, J.-E. Deschaud, B. Marcotegui, F. Goulette, L. Guibas, Kpconv: Flexible and deformable convolution for point clouds, in: *2019 IEEE/CVF International Conference on Computer Vision (ICCV)*, 2019, pp. 6410–6419. doi:10.1109/ICCV.2019.00651.
- [30] G. Qian, Y. Li, H. Peng, J. Mai, H. Hammoud, M. Elhoseiny, B. Ghanem, Pointnext: Revisiting pointnet++ with improved training and scaling strategies, in: S. Koyejo, S. Mohamed, A. Agarwal, D. Belgrave, K. Cho, A. Oh (Eds.), *Advances in Neural Information Processing Systems*, Vol. 35, 2022.
- [31] H. Zhou, Y. Feng, M. Fang, M. Wei, J. Qin, T. Lu, Adaptive graph convolution for point cloud analysis, in: *2021 IEEE/CVF International Conference on Computer Vision (ICCV)*, 2021, pp. 4945–4954. doi:10.1109/ICCV48922.2021.00492.
- [32] J. Choe, C. Park, F. Rameau, J. Park, I. S. Kweon, Pointmixer: Mlp-mixer for point cloud understanding, arXiv preprint arXiv:2111.11187 (2021).